View metadata, citation and similar papers at core.ac.uk

brought to you by CORE

provided by Elsevier - Publisher Connector

Interaction of Spin-Labeled Inhibitors of the Vacuolar H^+-ATPase with the Transmembrane V_o-Sector

Neil Dixon,[†] Tibor Páli,[*] Terence P. Kee,[†] Stephen Ball,[†] Michael A. Harrison,[†] John B. C. Findlay,[†] Jonas Nyman,[‡] Kalervo Väänänen,[‡] Malcolm E. Finbow,[§] and Derek Marsh[*]

[*]Max-Planck-Institut für biophysikalische Chemie, Abt. Spektroskopie, Göttingen, Germany; [†]University of Leeds, School of Chemistry and School of Biochemistry and Molecular Biology, Leeds, United Kingdom; [‡]University of Turku, Institute of Biomedicine, Department of Anatomy, Turku, Finland; and [§]Department of Biological and Biomedical Sciences, Glasgow Caledonian University, Glasgow, United Kingdom

ABSTRACT The osteoclast variant of the vacuolar H^+-ATPase (V-ATPase) is a potential therapeutic target for combating the excessive bone resorption that is involved in osteoporosis. The most potent in a series of synthetic inhibitors based on 5-(5,6-dichloro-2-indolyl)-2-methoxy-2,4-pentadienamide (INDOL0) has demonstrated specificity for the osteoclast enzyme, over other V-ATPases. Interaction of two nitroxide spin-labeled derivatives (INDOL6 and INDOL5) with the V-ATPase is studied here by using the transport-active 16-kDa proteolipid analog of subunit *c* from the hepatopancreas of *Nephrops norvegicus*, in conjunction with electron paramagnetic resonance (EPR) spectroscopy. Analogous experiments are also performed with vacuolar membranes from *Saccharomyces cerevisiae*, in which subunit *c* of the V-ATPase is replaced functionally by the *Nephrops* 16-kDa proteolipid. The INDOL5 derivative is designed to optimize detection of interaction with the V-ATPase by EPR. In membranous preparations of the *Nephrops* 16-kDa proteolipid, the EPR spectra of INDOL5 contain a motionally restricted component that arises from direct association of the indolyl inhibitor with the transmembrane domain of the proteolipid subunit *c*. A similar, but considerably smaller, motionally restricted population is detected in the EPR spectra of the INDOL6 derivative in vacuolar membranes, in addition to the larger population from INDOL6 in the fluid bilayer regions of the membrane. The potent classical V-ATPase inhibitor concanamycin A at high concentrations induces motional restriction of INDOL5, which masks the spectral effects of displacement at lower concentrations of concanamycin A. The INDOL6 derivative, which is closest to the parent INDOL0 inhibitor, displays limited subtype specificity for the osteoclast V-ATPase, with an IC_{50} in the 10-nanomolar range.

INTRODUCTION

Vacuolar H^+-ATPases are proton pumps that are responsible for the acidification of intracellular organelles (1). In the osteoclast variant, the vacuolar H^+-ATPase (V-ATPase) is located in a specialized region of the plasma membrane and induces acidification of the extracellular lacunae at the surface of the resorbing bone (2). Pathology in this remodeling of the bone leads to osteoporosis. Based on structure-function relationships for the macrolide antibiotics concanamycin and bafilomycin, which are specific inhibitors of the V-ATPases, Farina and colleagues have designed a series of synthetic inhibitors comprising the 5-(5,6-dichloro-2-indolyl)-2-methoxy-2,4-pentadienamide family (3–5). One of the most potent discovered so far is the 1,2,2,6,6-pentamethyl-piperidin-4-yl derivative, INDOL0 (see Fig. 1), which exhibits a selectivity for the osteoclast enzyme over other V-ATPases (6) and is found to be efficient in preventing bone loss in animal models of osteoporosis (7). Recently, we have synthesized two spin-labeled derivatives of this lead therapeutic compound (see Fig. 1) and characterized the interactions with lipid membranes by using electron paramagnetic resonance (EPR) spectroscopy (8,9). One derivative, INDOL6, is the nitroxide variant of the parent compound, INDOL0. The other derivative, INDOL5, is a spin-labeled analog that was designed to have EPR spectral properties optimized for the detection of interaction with the membrane-bound V-ATPase.

Spin-label EPR has been used widely to study the interactions of membrane-embedded proteins with the surrounding lipid-milieu (see, e.g., 10–13). Both stoichiometry and selectivity of lipid-protein interactions, and under favorable circumstances also lipid exchange rates, may be determined (14–18). Spin-labeled lipids have additionally been used to investigate the binding site for aminated local anesthetics as noncompetitive blockers of the nicotinic acetylcholine receptor (19). More direct information on interaction with the receptor has been obtained, however, by use of spin-labeled derivatives of the local anesthetics themselves (20). For all the above studies, it is necessary that the spin-labeled species interacting with the protein be resolved spectrally from that in the bulk lipid environment by virtue of its reduced rotational mobility. This can be achieved by varying the length of attachment of the spin-labeled group, as in INDOL5 and INDOL6 in Fig. 1. Guiding design principles

Submitted April 30, 2007, and accepted for publication September 4, 2007.

Address reprint requests to Dr. Derek Marsh, Tel.: 49-551-201-1285; E-mail: dmarsh@gwdg.de.

Tibor Páli's permanent address is Institute of Biophysics, Biological Research Centre, H-6701 Szeged, Hungary.

Abbreviations used: INDOL0, 5-(5,6-dichloro-2-indolyl)-2-methoxy-*N*-(1,2,2,6,6-pentamethylpiperidin-4-yl)-2,4-pentadienamide; INDOL5, (2*Z*,4*E*)-5-(5,6-dichloro-2-indolyl)-2-methoxy-*O*-[3-(2,2,5,5-tetramethylpyrolidinoxy)]-2,4-pentadienoic acid ester; INDOL6, (2*Z*,4*E*)-5-(5,6-dichloro-2-indolyl)-2-methoxy-*N*-[4-(2,2,6,6-tetramethylpiperidinoxy)]-2,4-pentadienamide.

Editor: David D. Thomas.

© 2008 by the Biophysical Society

0006-3495/08/01/506/09 $2.00

doi: 10.1529/biophysj.107.111781

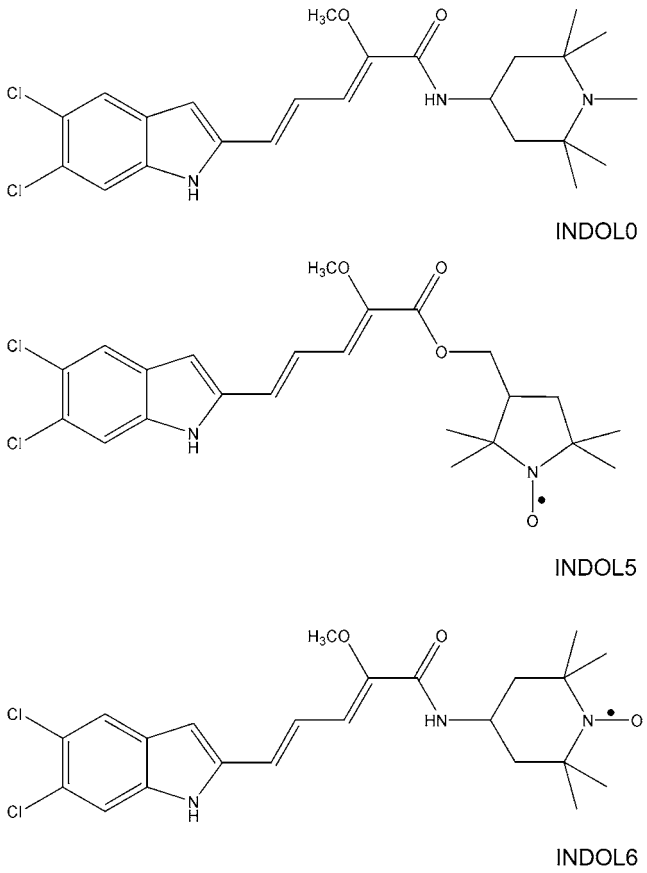

FIGURE 1 Chemical structures of 5-(2-indolyl)-2,4-pentadienoyl derivatives. INDOL0 is the parent inhibitor compound, and INDOL6 and INDOL5 are spin-labeled derivatives.

are offered by studies of lipid-protein interactions with spin labels located at different positions in the lipid chain (21–23). The ability to resolve the spectral components is determined by the flexibility of the spin-label attachment in the fluid lipid environment, and not by the thermodynamic affinity of the spin-labeled species for the protein. Both the latter and the stoichiometry of interaction determine the relative proportions of the two components, which are quantitated by difference spectroscopy (24).

In this work, we investigate the interaction of the spin-labeled indolyl inhibitors with the V-ATPase in yeast vacuolar membranes, and in membranes from the hepatopancreas of *Nephrops norvegicus* that contain almost exclusively the 16-kDa proteolipid analog of the V-ATPase *c*-subunit. In the yeast vacuolar membranes, the native *c*-subunit that is encoded by the *VMA3* gene is replaced by recombinant 16-kDa *Nephrops* proteolipid to produce a transport-competent V-ATPase (25,26). Direct interactions of the spin-labeled inhibitors with the transmembrane V_o-sector of the enzyme are detected by EPR spectroscopy, in a manner similar to that used previously to study the association of spin-labeled local anesthetics with the nicotinic acetylcholine receptor (20). These studies are augmented by investigation of the effects of the classical V-ATPase inhibitor concanamycin A on the interaction with the inhibitor spin labels. This EPR investigation with spin-labeled inhibitors complements that conducted previously on the interaction of the unlabeled V-ATPase inhibitors, concanamycin A and INDOL0, as registered by EPR spectroscopy of the site-specifically spin-labeled protein (27). In addition, we have characterized the subtype selectivity of V-ATPase inhibition by the spin-labeled (2-indolyl)-pentadienes, by using microsomes derived from chicken medullary bone and from chicken brain, in addition to yeast vacuoles.

MATERIALS AND METHODS

Materials

Concanamycin A was obtained from Fluka (Buchs, Switzerland). Dimyristoyl phosphatidylcholine was from Avanti Polar Lipids (Alabaster, AL). The inhibitor INDOL0 (also known as SB 242754) was synthesized according to the literature (3,6). Spin-labeled 5-(5,6-dichloro-2-indolyl)-2,4-pentadienoyl inhibitors INDOL6 and INDOL5 (see Fig. 1) were synthesized as described in Dixon et al. (9). The *Saccharomyces cerevisiae* W303-1B vatc cells (*MATα ade2*, *ura3*, *leu2 his3*, *trp1*, Δ*vma3*::*LEU2*) were a kind gift of Nathan Nelson, University of Tel-Aviv (25).

Isolation of 16-kDa membranes and vacuolar membranes

Endogenous membranes containing the 16-kDa channel proteolipid were prepared from the hepatopancreas of the decapod *Nephrops norvegicus* by extraction with *n*-lauryl sarcosine, or with 20 mM NaOH, according to the procedures in the literature ((28–30) and (31,32), respectively). These membranous preparations contain the endogenous lipids, but the amount of lipid is strongly reduced in the preparations extracted with *N*-lauroyl sarcosine (33). EDTA-washed yeast vacuolar membranes transfected with *Nephrops* 16-kDa proteolipid were prepared as described in Uchida et al. (34). Proteolipid refers here to the classical definition of a hydrophobic protein; it does not imply lipoylation.

Spin-labeling

Membranes, either *Nephrops* 16-kDa membranes or yeast vacuolar membranes, were suspended in 50 mM borate buffer with 10 mM NaCl, pH 9.0, or in 50 mM HEPES buffer with 10 mM NaCl and 10 mM EDTA, at pH 7.8, respectively. Spin-labeled inhibitors were added to membranes (~1 mg membrane protein) in 500 μl of buffer from concentrated solutions in <10 μl dimethyl sulfoxide (DMSO). Nominal spin-labeled inhibitor to protein mole ratio was 1:1 or less (for 16-kDa membranes). When required, concanamycin A was added similarly in concentrated DMSO solution. After incubation for 30 min, membranes were packed in 1-mm i.d. glass capillaries by pelleting in a benchtop centrifuge. Sample length was trimmed to 5 mm, excess supernatant was removed, and the capillary was flame-sealed.

EPR spectroscopy

EPR spectra were recorded on a Bruker EMX 9-GHz spectrometer (Rheinstetten, Germany). Sample capillaries were accommodated in standard quartz EPR tubes that contained light silicone oil for thermal stability. Temperature was regulated by thermostated nitrogen gas-flow, and measured with a fine-wire

thermocouple situated in the silicone oil at the top of the microwave cavity. Analysis of two-component EPR spectra was performed as described in Páli et al. (33), using a spectral library obtained from spin-labeled small unilamellar vesicles of dimyristoyl phosphatidylcholine (35). In spectral addition, the whole of the two-component experimental spectrum was fitted first, and then the relative weights of the two components were optimized on the low-field hyperfine lines. Note that choosing the best-matching fluid component from a spectral library corrects not only for perturbations of the bulk lipid mobility by the presence of the protein, but also largely corrects for any lifetime broadening that arises from exchange on and off the protein (see, e.g., (36)). Comparison of the results of spectral subtraction with spectral simulations for two-site exchange shows that this subtraction protocol largely corrects for the effects of exchange and yields reliable values for the relative proportions of the two spectral components (12,17,37). If, at the same lipid/protein ratio, f_1 and f_2 are the fractions of two motionally restricted spin-labeled species that compete for the same sites on the protein, then the ratio of their average association constants (K_1/K_2) is given by $K_1/K_2 = (1/f_2–1)/(1/f_1–1)$ (24).

Measurement of V-ATPase activity in yeast

V-ATPase was purified from yeast vacuolar membranes solubilized in dodecyl maltoside on discontinuous glycerol gradients, essentially according to Uchida et al. (34). ATPase activity was assayed at 30°C by colorimetric development of phosphate release using ammonium molybdate, as described in Harrison et al. (26).

Measurement of V-ATPase H^+-transport in bone-derived microsomes

Chicken medullary bone-derived microsomes from regularly egg-laying hens were prepared as described in Väänänen et al. (38), and the fluorescence-quench method with acridine orange was used to monitor microsome acidification. The microsomes were diluted in a buffer containing 150 mM KCl, 5 mM $MgSO_4$, 1.5 μM acridine orange, 1 μM valinomycin, and 5 mM HEPES/Tris, pH 7.4, and aliquoted in a 96-well plate. Inhibitors were added in DMSO (1% final concentration) and incubated for 20–40 min before fluorescence measurement in a microtiter plate reader (Cameleon, Hidex, Finland). Acidification was initiated by addition of ATP to a final concentration of 5 mM. Six wells were treated simultaneously: control and five different concentrations of inhibitor. Readings of acridine orange fluorescence (480 nm excitation, 535 nm emission) were taken every 30 s. At the end of the assay, nigericin was added (10 μg/ml final concentration) to confirm that a transmembrane proton gradient had been established. For calculation of the percentage inhibition, the initial linear slope of the fluorescence-time curve was used to determine the rate of acidification. For comparison, assays were also performed with brain microsomes derived from chicken cerebrum and cerebellum. These were prepared by methods similar to those for the osteoclast microsomes.

Sequence alignments

Amino-acid sequences were taken from the PIR Database. Sequence alignments were performed with CLUSTAL W (39) and displayed with the PIR alignment viewer.

RESULTS AND DISCUSSION

Experiments with spin-labeled inhibitors were performed using membranous preparations of the 16-kDa proteolipid subunit from *Nephrops norvegicus*, which contain almost exclusively the analog of vacuolar subunit *c*, at high concentration. Corresponding experiments were also performed on yeast vacuolar membranes in which the endogenous subunit *c* of the V-ATPase was replaced by the *Nephrops* 16-kDa proteolipid. Inhibition studies were carried out both with purified yeast vacuolar membranes, and with microsomes prepared from chicken medullary bone and from chicken brain tissue.

The strong degree of homology between V-ATPase subunits-*c* from different species ensures the relevance of these experimental systems. This is illustrated by the fact that the 16-kDa proteolipid from *Nephrops* substitutes for subunit *c* in yeast (25,26). As seen from the alignments in Fig. 2, the yeast V-ATPase subunit *c* has 69% identity with the *Nephrops* protein, and the human subunit *c* has 80% identity with *Nephrops*. Also, a putative protein from chicken has 81% identity with *Nephrops* 16-kDa proteolipid.

Nephrops 16-kDa proteolipid membranes

Fig. 3 shows the temperature dependence of the EPR spectra from 16-kDa proteolipid membranes to which the spin-labeled inhibitor INDOL5 has been added. At intermediate and higher temperatures, the EPR spectra clearly consist of two components. The relatively sharp, three-line spectral component, the outer lines of which are indicated by dashed arrows, is assigned to the mobile population of INDOL5 spin-labels in fluid bilayer regions of the membrane. This assignment is

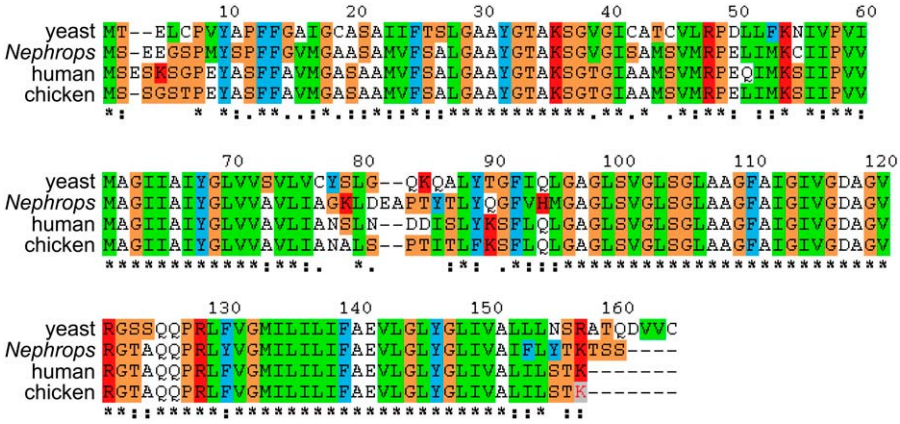

FIGURE 2 Alignment of the amino-acid sequences for the 16-kDa proteolipid, V-ATPase subunit *c* from different species. Data are taken from the PIR database with the following Uniprot KB accession codes: human, P27449; chicken, Q5ZJ19; *Nephrops*, Q26250; yeast, P25515.

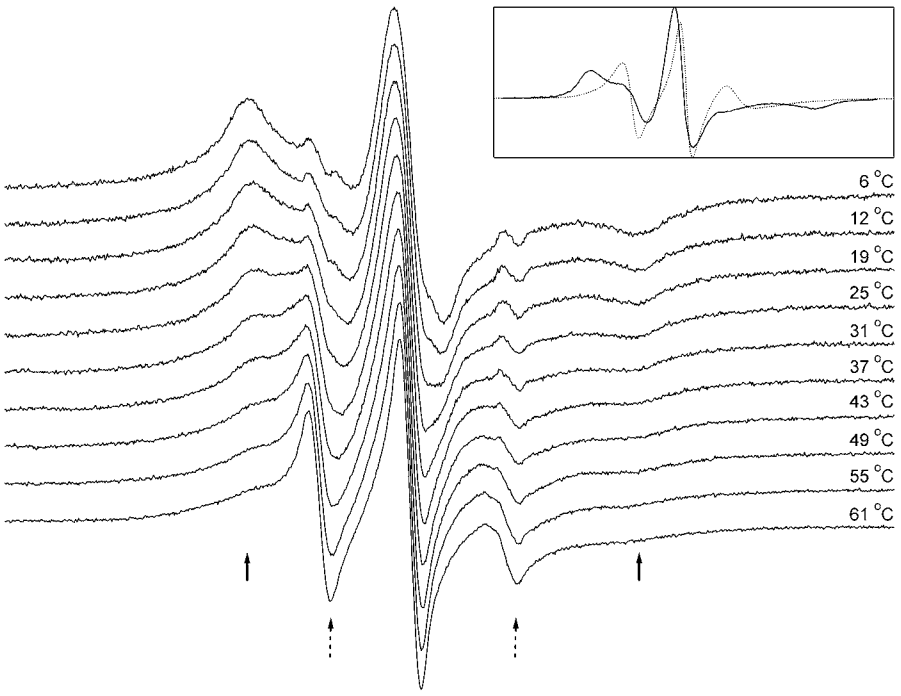

FIGURE 3 EPR spectra of spin-labeled indole, INDOL5, in 16-kDa proteolipid membranes from *Nephrops norvegicus*. Spectra were recorded at the temperatures indicated in the figure. The spectral component from the motionally restricted population of INDOL5 is indicated by solid arrows; that from the mobile (fluid-bilayer) component is indicated by dashed arrows. The small, sharp component that appears close to the position of the dashed arrows in the spectrum at 6°C arises from free, aqueous spin label. Total scan width = 150 G. (*Inset*) The single-component spectra at 43°C.

made by comparison with the single EPR spectral component that is observed in fluid bilayer membranes composed of phospholipid alone (9). The broad component that is resolved in the outer wings of the spectrum, and is indicated by the solid arrows in Fig. 3, is therefore assigned to the population of spin-labeled INDOL5 inhibitors that are restricted in their motion by interacting directly with the protein. Because the 16-kDa proteolipid does not project appreciably from the membrane surface (25,33), the INDOL5 spin label must be associated, therefore, with the transmembrane section of the 16-kDa subunit *c*.

The spin-labeled indole derivative INDOL5 was designed specifically to optimize resolution of the two-component EPR spectra in *Nephrops* membranes, which contain a high concentration of cholesterol and have a high protein density (see (9)). Resolution of the two spectral components is achieved at temperatures of 37°C and higher. At lower temperatures, the mobility of the lipid chains in the bilayer regions of the membrane is reduced considerably, and the spectrum of INDOL5 in these regions then strongly overlaps that of INDOL5 associated directly with the protein. EPR spectra of the latter are not as strongly temperature-dependent because they lie in the slow-motion regime of nitroxide EPR spectroscopy. At 6°C, they resemble an anisotropic powder pattern, with small, sharp lines superimposed that arise from a small amount of free, aqueous spin label. Note that the 16-kDa proteolipid is an extremely heat-stable protein (25).

The fraction of INDOL5 spin label that gives rise to the broad, motionally restricted component in the spectra of Fig. 3, at 43°C and above, was determined by comparison with library spectra that best matched each of the two components. Linear combinations of the single-component spectra (see *inset* to Fig. 3) were fitted to the two-component experimental spectra. Approximately 66 ± 3% of the INDOL5 spin label is motionally restricted by direct interaction with the 16 kDa protein (mean over 43–61°C). For comparison, it was found previously that 60–70% of spin-labeled phosphatidylcholine was motionally restricted in similar 16-kDa proteolipid membranes from *Nephrops* (33). Thus, the spin-labeled indole inhibitor either samples the whole of the hydrophobic surface of the 16-kDa protein that is available to lipid in these closely packed membranes, or it is restricted to a more limited number of sites at the lipid-protein interface, for which it exhibits a higher specificity. Experiments at probe concentrations are unable to distinguish between these two possibilities (see, e.g., (36,40)). For alkali-extracted 16-kDa membranes from *Nephrops*, in which the protein is less densely packed, ~60% of spin-labeled INDOL5 is motionally restricted, whereas only ~30% of spin-labeled phosphatidylcholine is motionally restricted in such membranes (33). This implies a selectivity for the spin-labeled indole that is characterized by an approximately fourfold greater average association constant compared with phosphatidylcholine (see Materials and Methods and (24)). It should be remembered that modest values of the relative association constants in membrane systems can achieve the same degree of occupancy as much larger binding constants (in mole fraction units) in solution, because of the reduction in dimensionality in membranes (41).

Note that, at the highest temperatures of measurement, the linewidths of the component from spin labels in the fluid lipid environment are still relatively broad. The peak-to-peak linewidth of the diagnostic low-field line is $\Delta H_{pp}^{(f)} \sim 4$ G. This considerably exceeds the line-broadening that might be produced by exchange effects. The intrinsic exchange rates

of spin-labeled phospholipids that display no selectivity of lipid-protein interaction are in the range $\tau_b^{-1} \sim 10^7 s^{-1}$ for various membrane proteins (24). This is almost an order-of-magnitude slower than diffusional lipid exchange in fluid bilayers: $\tau_{diff}^{-1} \sim 10^8 s^{-1}$ (42,43). For comparable populations of free and protein-associated spin labels (i.e., $\tau_f^{-1} \sim \tau_b^{-1}$), the contribution of molecular exchange to the low-field linewidth of the free component is therefore maximally $\delta\Delta H_{pp}^{(f)} = (2/\sqrt{3})(\hbar/g\beta)\tau_f^{-1} \sim 0.7$ G (see (36)). Additionally, as noted already in Materials and Methods, the fitting strategy of choosing the best fitting fluid component from a library of phosphatidylcholine-vesicle spectra largely corrects for contributions to the linewidth from exchange. The result is that relative populations of the spin-label species are estimated reliably by this strategy.

Yeast vacuolar membranes

Fig. 4 shows the temperature dependence of the EPR spectra from yeast vacuolar membranes to which the spin-labeled inhibitor INDOL6 has been added. At low temperatures, the spectral extent or anisotropy is less than that of INDOL5, even though the latter spin-labeled derivative possesses greater intrinsic segmental mobility (9). Table 1 gives values of the outer hyperfine splitting, $2A_{max}$, of both INDOL6 and INDOL5 derivatives in *Nephrops* membranes and vacuolar membranes, and in lipid bilayer membranes of dimyristoyl phosphatidylcholine. From this, the higher rotational mobility of INDOL5, which gives rise to a greater motional averaging of the outer hyperfine splitting than that of INDOL6, is evident in both *Nephrops* membranes and dimyristoyl phosphatidylcholine bilayers. The smaller values of $2A_{max}$ for INDOL6 in yeast vacuolar membranes, relative to those in *Nephrops* membranes, reflect the higher lipid mobility and the lower intramembranous protein density in the vacuolar membranes.

Although the resolution is not as good as in Fig. 3, a small motionally restricted component is present in the outer wings of the EPR spectra of INDOL6 in vacuolar membranes. The position of this component is indicated by the dotted lines in Fig. 4 (see also *inset*). It is evident as an asymmetry of the high-field peak at lower temperatures, and as a shoulder on the low-field peak at intermediate temperatures. As in *Nephrops* membranes, this motionally restricted component is attributed to a population of INDOL6 that is interacting directly with the membrane protein. The intensity is lower than that of the motionally restricted component in Fig. 3, because of the lower intramembranous protein density in the vacuolar membranes. In view of the highly hydrophobic nature of INDOL6, as evidenced by the interaction with lipid membranes (9), and by analogy with the motional restriction of spin-labeled lipids in *Nephrops* membranes (33) and spin-labeled local anesthetics in *Torpedo* membranes (20), this motionally restricted population of INDOL6 is also associated with the transmembrane protein domains in vacuolar membranes, particularly those of the V-ATPase.

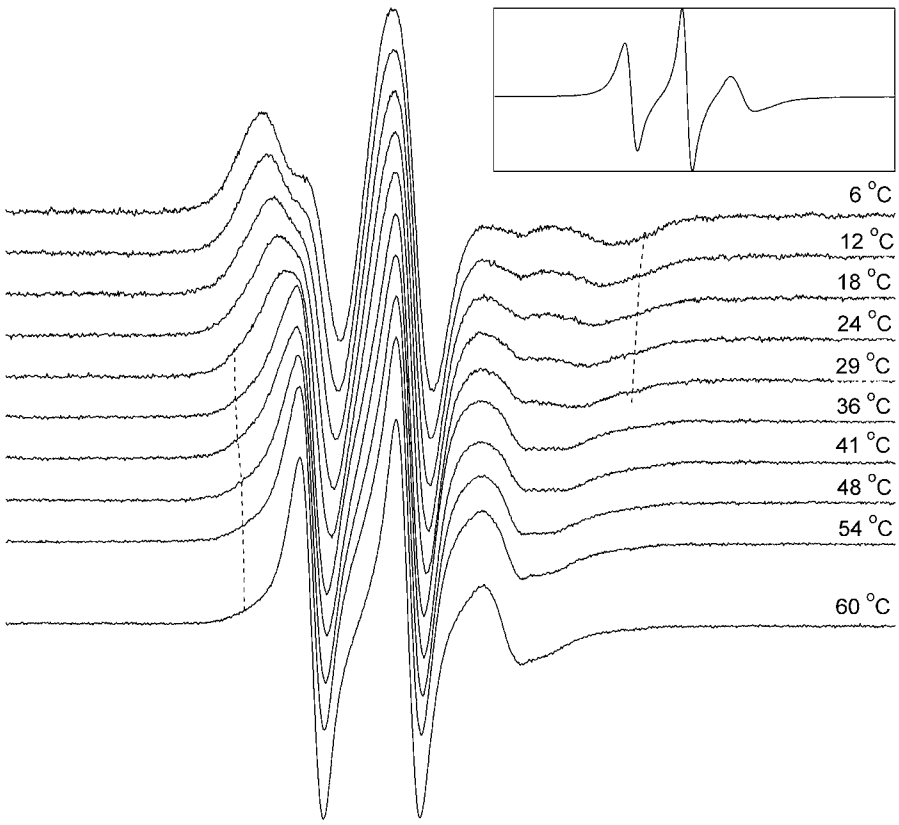

FIGURE 4 EPR spectra of spin-labeled indole, INDOL6, in yeast vacuolar membranes. Spectra were recorded at the temperatures indicated in the figure. The spectral component from the motionally restricted population of INDOL6 is indicated by the vertical dotted lines. Total scan width = 150 G. (*Inset*) The single-component fluid spectrum at 60°C.

TABLE 1 Temperature dependence of the outer hyperfine splitting, $2A_{max}$ (Gauss), in the EPR spectra of the INDOL6 and INDOL5 spin-labeled V-ATPase inhibitors in *Nephrops* 16-kDa proteolipid membranes, and yeast vacuolar membranes, and in dimyristoyl phosphatidylcholine bilayer membranes

Inhibitor	6°C	24°C	40°C
Nephrops 16-kDa			
INDOL6	67.9	65.7	64.0
INDOL5	65.6	64.5	62.5,* 37†
Yeast vacuolar			
INDOL6	59.8	52.2	45.1
Dimyristoyl phosphatidylcholine			
INDOL6	60.1	53.5	47.1
INDOL5	58.2	45.7	34.5

*Motionally restricted component.
†Fluid component.

Spin-labeled inhibitors in the presence of concanamycin A

Fig. 5 shows the EPR spectra of INDOL5 in *Nephrops* 16-kDa proteolipid membranes in the presence of concanamycin A, at various temperatures. The amounts of concanamycin A added were: 0:1, 1:1, and 5:1 mol/mol, relative to INDOL5. Adding an equimolar amount of concanamycin A, relative to spin-labeled inhibitor, produces little difference in the relative population of motionally restricted INDOL5 (see *dotted lines* in Fig. 5). However, adding an excess of concanamycin A produces a pronounced increase in the population of motionally restricted INDOL5 (*dashed lines* in Fig. 5). The latter is an effect that is shared also with spin-labeled lipids, the motionally restricted population of which is increased on adding concanamycin A to 16-kDa membranes (data not shown). This general feature of the interactions of concanamycin A with these membranes tends to mask any displacement of the indole inhibitor by concanamycin.

Quantification of the spectra shown in Fig. 5, and others at intermediate temperatures, was performed by fitting a linear combination of library spectral components to each two-component spectrum. In the absence of concanamycin A, the fraction of motionally restricted INDOL5 spin label is $f = 0.66 \pm 0.03$, and that in the presence of equimolar concanamycin A is $f = 0.64 \pm 0.03$. Increasing the concanamycin A concentration fivefold, however, increases the fraction of motionally restricted INDOL5 to $f = 0.78 \pm 0.03$. That INDOL5 should be displaced from the inhibitory site by concanamycin A can be inferred from studies of their relative potencies that are given later. This suggests that displacement of INDOL5 is compensated in the EPR spectrum by the additional immobilizing potential of concanamycin A that comes to dominate at higher concentrations. Varying the concentration of concanamycin A in the lower range has failed to reveal a window where the displacement dominates. Previous data on the site-specifically labeled protein suggest that the indole inhibitors compete with concanamycin A for similar sites on the transmembrane domain of the 16-kDa proteolipid subunit *c* (27).

Fig. 6 shows the EPR spectra of INDOL6 in yeast vacuolar membranes in the presence of concanamycin A, at various temperatures. The amount of concanamycin A added was 0:1 and 2:1 mol/mol, relative to INDOL6. The effect of concanamycin A in increasing the population of motionally restricted species is also evident here, for INDOL6 in yeast vacuolar membranes. Competition would not be observed in this experiment, because of the low intrinsic population of motionally restricted INDOL6 in vacuolar membranes (see above).

Inhibition assays

To compare the inhibitory potency of the spin-labeled indole compounds with that of the parent INDOL0, we prepared

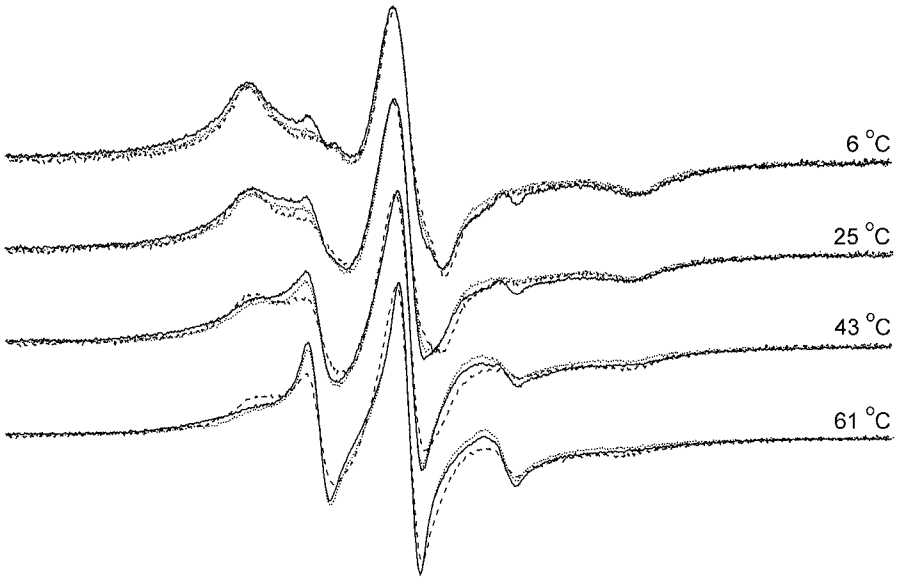

FIGURE 5 EPR spectra of spin-labeled indole, INDOL5 (150 μM), in *Nephrops* 16-kDa proteolipid membranes to which concanamycin A was added. (*Solid line*) No concanamycin A; (*dotted line*) 150 μM concanamycin A; (*dashed line*) 750 μM concanamycin A. Spectra were recorded at the temperatures indicated in the figure. Total scan width = 150 G.

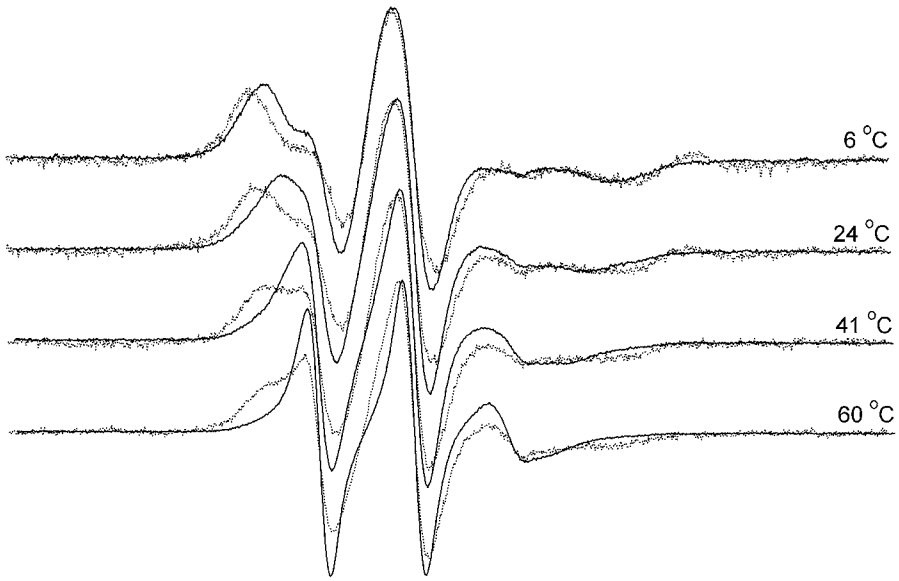

FIGURE 6 EPR spectra of spin-labeled indole, INDOL6 (25 μM), in yeast vacuolar membranes to which concanamycin A was added. (*Solid line*) No concanamycin A; (*dashed line*) 50 μM concanamycin A. Spectra were recorded at the temperatures indicated in the figure. Total scan width = 150 G.

microsomes from medullary bone of regularly egg-laying hens, which is a source rich in osteoclasts. For additional comparison, we also used microsomes prepared from chicken brain tissue. Acidification of the microsomes was detected as the quenching of fluorescence from entrapped acridine orange. The fluorescence quenching was fully inhibited by 30 nM bafilomycin, confirming that the H^+-uptake observed was mediated by the V-ATPase. Fig. 7 shows the inhibition curves for the three indole compounds, and for bafilomycin A1, that are obtained with chicken medullary bone microsomes (*upper panel*), and with chicken brain microsomes (*lower panel*). Indole concentrations required for 50% inhibition are listed in Table 2. The IC_{50} values for the parent compound, INDOL0, are ~20 nM and 100 nM for acidification of bone-and brain-derived microsomes, respectively. This pronounced selectivity for the osteoclast enzyme is in agreement with previous observations by Nadler et al. (6), who analyzed selectivity by using microsomes from chicken medullary bone and chicken adrenal glands.

The spin-labeled derivative INDOL6 is at least as potent as the parent compound in bone microsomes ($IC_{50} \approx 15$ nM), and apparently more potent than INDOL0 in brain microsomes ($IC_{50} \approx 20$ nM). Correspondingly, however, INDOL6 displays a reduced selectivity for the osteoclast enzyme relative to the brain enzyme, as compared with that of INDOL0 (see Table 2). The other spin-labeled derivative, INDOL5, is far less potent an inhibitor than is INDOL6, with an IC_{50} of ~5 μM for both bone-derived and brain-derived microsomes. This latter spin-labeled derivative was chosen for its spectroscopic properties in *Nephrops* 16-kDa proteolipid membranes, which contain only subunit *c*, at high concentration.

Inhibition of V-ATPase activity was also assayed using purified vacuolar membranes from *Saccharomyces cerevisiae* in which the endogenous subunit *c* was replaced by the *Nephrops* 16-kD proteolipid. Fig. 8 shows inhibition curves for the indole inhibitors, and for concanamycin A. The inhibitory potencies of the indole derivatives differ from those for the osteoclast enzyme. The IC_{50} for INDOL0 is ~13 nM and

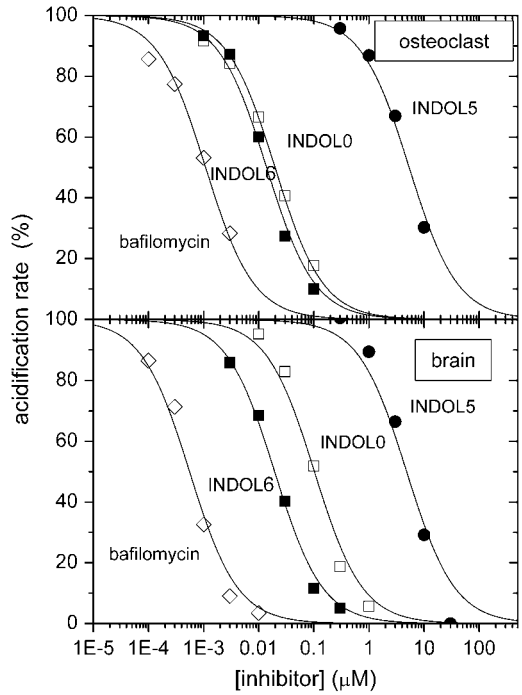

FIGURE 7 Inhibitor profile of V-ATPase H^+-transport activity in chicken medullary bone microsomes (*upper panel*) and chicken brain microsomes (*lower panel*). Activity in the presence of inhibitors is shown as percentage of the initial rate of internal acidification, relative to that in the absence of inhibitors. (*Open squares*) INDOL0; (*solid squares*) INDOL6; (*circles*) INDOL5; and (*diamonds*) bafilomycin A1.

TABLE 2 Inhibitory concentrations, IC_{50} (nM), of indole derivatives and bafilomycin/concanamycin for vacuolar H^+-ATPase in chicken medullary bone (osteoclast) and brain microsomes, and for V-ATPase in yeast vacuoles

Inhibitor	Osteoclast	Brain	Yeast
Bafilomycin/concanamycin*	1.1 ± 0.1	0.56 ± 0.07	5 ± 1
INDOL0	20 ± 1	105 ± 15	13 ± 2
INDOL6	14 ± 1	20 ± 1	4000 ± 1000
INDOL5	5400 ± 500	4800 ± 1100	—

*Concanamycin A for yeast, otherwise bafilomycin A1.

that for INDOL6 is 4 ± 1 μM, i.e., the spin-labeled derivative is far less potent in yeast than is the parent compound. No inhibition was found for INDOL5 at 100 μM; therefore the IC_{50} for this indole must lie at least in the millimolar range, when assayed with yeast vacuolar membranes (data not shown). This reduction in potency for INDOL5 is at least comparable to that in the bone-derived microsomes. Note that the 5000-fold lower IC_{50} of concanamycin relative to INDOL5 should ensure displacement of the latter by equimolar concanamycin. This supports our interpretation of the EPR data: that the displacement is masked by the additional immobilizing potential of concanamycin.

The spin-label derivatives INDOL6 and INDOL5 exhibit a pronounced subtype specificity for inhibition of the osteoclast V-ATPase over that of the yeast enzyme. Also, INDOL6 does not exhibit any reduction in potency relative to the parent INDOL0 for inhibition of the osteoclast V-ATPase, unlike the situation with the yeast enzyme. (Note that the human V-ATPase subunit *c* bears 80% identity to the *Nephrops* 16-kDa proteolipid, as does the putative protein identified from chicken; see Fig. 2.) Bioavailability, however, may play a significant role in any inter-species comparison. This is illustrated, for instance, by the fact that INDOL0 inhibits yeast V-ATPase purified on glycerol gradients ($IC_{50} \approx 3.5 \pm 1$ nM; (44)) more potently than it does in vacuolar membrane preparations ($IC_{50} \approx 13$ nM).

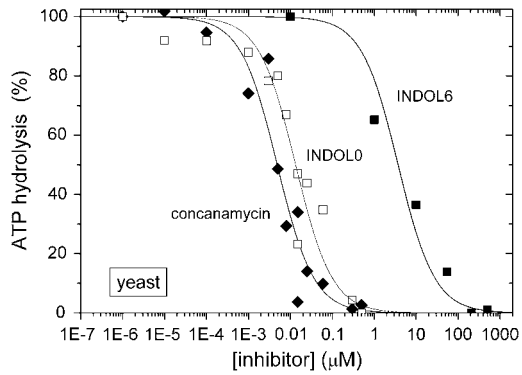

FIGURE 8 Inhibitor profile of ATPase activity in V-ATPase from yeast vacuolar membranes expressing *Nephrops* 16-kDa proteolipid. ATP hydrolysis is shown as the percentage of that in the absence of inhibitors. (*Open squares*) INDOL0; (*solid squares*) INDOL6; and (*diamonds*) concanamycin A.

CONCLUSIONS

The spin-labeled indolyl inhibitors allow direct demonstration of the association of this class of compounds with the transmembrane domain of the V-ATPase proteolipid subunit *c*. This is achieved by means of a specific, motionally broadened, anisotropic component that is resolved in their EPR spectrum. Attempts to demonstrate displacement of INDOL5 by concanamycin A were unsuccessful because of the intrinsic immobilizing effect of concanamycin. Our previous results with spin-labeled 16-kDa proteolipid suggest that the sites for both inhibitors are close to the glutamic acid residue E140 that is essential for proton translocation (27). The specificity found for the osteoclast V-ATPase, relative to yeast, indicates that the spin-labeled INDOL6 inhibitor could be used to explore the basis for functional selectivities. This subtype selectivity extends also to the INDOL5 spin-label derivative (but not relative to chicken brain, in the latter case).

We thank Mrs. M. Scott for the preparation of *Nephrops* membranes and Frau B. Angerstein for technical assistance.

This work was supported by contract No. QLG-CT-2000-01801 of the European Commission.

REFERENCES

1. Nishi, T., and M. Forgac. 2002. The vacuolar H^+-ATPases—nature's most versatile proton pumps. *Nat. Rev. Mol. Cell Biol.* 3:94–103.
2. Sun-Wada, G. H., Y. Wada, and M. Futai. 2003. Vacuolar H^+ pumping ATPases in luminal acidic organelles and extracellular compartments: common rotational mechanism and diverse physiological roles. *J. Bioenerg. Biomembr.* 35:347–358.
3. Gagliardi, S., G. Nadler, E. Consolandi, C. Parini, M. Morvan, M. N. Legave, P. Belfiore, A. Zocchetti, G. D. Clarke, I. James, P. Nambi, M. Gowen, and C. Farina. 1998. 5-(5,6-dichloro-2-indolyl)-2-methoxy-2,4-pentadienamides: novel and selective inhibitors of the vacuolar H^+-ATPase of osteoclasts with bone antiresorptive activity. *J. Med. Chem.* 41:1568–1573.
4. Farina, C., S. Gagliardi, G. Nadler, M. Morvan, C. Parini, P. Belfiore, L. Visentin, and M. Gowen. 2001. Novel bone antiresorptive agents that selectively inhibit the osteoclast V-H^+-ATPase. *Farmaco.* 56:113–116.
5. Farina, C., and S. Gagliardi. 2002. Selective inhibition of osteoclast vacuolar H^+-ATPase. *Curr. Pharm. Des.* 8:2033–2048.
6. Nadler, G., M. Morvan, I. Delimoge, P. Belfiore, A. Zocchetti, I. James, D. Zembryki, E. Lee-Rycakzewski, C. Parini, E. Consolandi, S. Gagliardi, and C. Farina. 1998. (2*Z*,4*E*)-5-(5,6-dichloro-2-indolyl)-2-methoxy-*N*-(1,2,2,6,6-pentamethylpiperidin-4-yl)-2,4-pentadienamide, a novel, potent and selective inhibitor of the osteoclast V-ATPase. *Bioorg. Med. Chem. Lett.* 8:3621–3626.
7. Visentin, L., R. A. Dodds, M. Valente, P. Misiano, J. N. Bradbeer, S. Oneta, X. Liang, M. Gowen, and C. Farina. 2000. A selective inhibitor of the osteoclastic V-H^+-ATPase prevents bone loss in both thyroparathyroidectomized and ovariectomized rats. *J. Clin. Invest.* 106:177–179.
8. Dixon, N., T. Páli, S. Ball, M. A. Harrison, D. Marsh, J. B. C. Findlay, and T. P. Kee. 2003. New biophysical probes for structure-activity analyses of vacuolar-H^+-ATPase enzymes. *Org. Biomol. Chem.* 1:4361–4363.
9. Dixon, N., T. Páli, T. P. Kee, and D. Marsh. 2004. Spin-labeled vacuolar-ATPase inhibitors in lipid membranes. *Biochim. Biophys. Acta.* 1665:177–183.
10. Marsh, D., A. Watts, and F. J. Barrantes. 1981. Phospholipid chain immobilization and steroid rotational immobilization in acetylcholine receptor-rich membranes from *Torpedo marmorata*. *Biochim. Biophys. Acta.* 645:97–101.

11. Esmann, M., and D. Marsh. 1985. Spin-label studies on the origin of the specificity of lipid-protein interactions in Na^+,K^+-ATPase membranes from *Squalus acanthias*. *Biochemistry.* 24:3572–3578.
12. Ryba, N. J. P., L. I. Horváth, A. Watts, and D. Marsh. 1987. Molecular exchange at the lipid-rhodopsin interface: spin-label electron spin resonance studies of rhodopsin-dimyristoyl phosphatidylcholine recombinants. *Biochemistry.* 26:3234–3240.
13. Horváth, L. I., P. J. Brophy, and D. Marsh. 1990. Influence of polar residue deletions on lipid-protein interactions with the myelin proteolipid protein. Spin-label ESR studies with DM-20/lipid recombinants. *Biochemistry.* 29:2635–2638.
14. Marsh, D. 1997. Stoichiometry of lipid-protein interaction and integral membrane protein structure. *Eur. Biophys. J.* 26:203–208.
15. Páli, T., D. Bashtovyy, and D. Marsh. 2006. Stoichiometry of lipid interaction with transmembrane proteins, deduced from the 3-D structures. *Protein Sci.* 15:1153–1161.
16. Horváth, L. I., P. J. Brophy, and D. Marsh. 1988. Influence of lipid headgroup on the specificity and exchange dynamics in lipid-protein interactions. A spin label study of myelin proteolipid apoprotein-phospholipid complexes. *Biochemistry.* 27:5296–5304.
17. Horváth, L. I., P. J. Brophy, and D. Marsh. 1988. Exchange rates at the lipid-protein interface of myelin proteolipid protein studied by spin-label electron spin resonance. *Biochemistry.* 27:46–52.
18. Horváth, L. I., P. J. Brophy, and D. Marsh. 1993. Exchange rates at the lipid-protein interface of the myelin proteolipid protein determined by saturation transfer electron spin resonance and continuous wave saturation studies. *Biophys. J.* 64:622–631.
19. Mantripragada, S., L. I. Horváth, H. R. Arias, G. Schwarzmann, K. Sandhoff, F. J. Barrantes, and D. Marsh. 2003. Lipid-protein interactions and effect of local anesthetics in acetylcholine receptor-rich membranes from *Torpedo marmorata* electric organ. *Biochemistry.* 42:9167–9175.
20. Horváth, L. I., H. R. Arias, H. O. Hankovszky, K. Hideg, F. J. Barrantes, and D. Marsh. 1990. Association of spin-labeled local anesthetics at the hydrophobic surface of acetylcholine receptor in native membranes from *Torpedo marmorata*. *Biochemistry.* 29:8707–8713.
21. Pates, R. D., and D. Marsh. 1987. Lipid mobility and order in bovine rod outer segment disk membranes. A spin-label study of lipid-protein interactions. *Biochemistry.* 26:29–39.
22. Marsh, D., and F. J. Barrantes. 1978. Immobilized lipid in acetylcholine receptor-rich membranes from *Torpedo marmorata*. *Proc. Natl. Acad. Sci. USA.* 75:4329–4333.
23. Esmann, M., A. Watts, and D. Marsh. 1985. Spin-label studies of lipid-protein interactions in (Na^+,K^+)-ATPase membranes from rectal glands of *Squalus acanthias*. *Biochemistry.* 24:1386–1393.
24. Marsh, D., and L. I. Horváth. 1998. Structure, dynamics and composition of the lipid-protein interface. Perspectives from spin-labeling. *Biochim. Biophys. Acta.* 1376:267–296.
25. Holzenburg, A., P. C. Jones, T. Franklin, T. Páli, T. Heimburg, D. Marsh, J. B. C. Findlay, and M. E. Finbow. 1993. Evidence for a common structure for a class of membrane channels. *Eur. J. Biochem.* 213:21–30.
26. Harrison, M. A., P. C. Jones, Y. I. Kim, M. E. Finbow, and J. B. C. Findlay. 1994. Functional properties of a hybrid vacuolar H^+-ATPase in *Saccharomyces* cells expressing the *Nephrops* 16-kDa proteolipid. *Eur. J. Biochem.* 221:111–120.
27. Páli, T., G. Whyteside, N. Dixon, T. P. Kee, S. Ball, M. A. Harrison, J. B. C. Findlay, M. E. Finbow, and D. Marsh. 2004. Interaction of inhibitors of the vacuolar H^+-ATPase with the transmembrane V_o-sector. *Biochemistry.* 43:12297–12305.
28. Finbow, M. E., T. E. J. Buultjens, N. J. Lane, J. Shuttleworth, and J. D. Pitts. 1984. Isolation and characterization of arthropod gap junctions. *EMBO J.* 3:2271–2278.
29. Finbow, M. E., E. E. Eliopoulos, P. J. Jackson, J. N. Keen, L. Meagher, P. Thompson, P. C. Jones, and J. B. C. Findlay. 1992. Structure of 16 kDa integral membrane protein that has identity to the putative proton channel of the vacuolar H^+-ATPase. *Protein Eng.* 5:7–15.
30. Buultjens, T. E. J., M. E. Finbow, N. J. Lane, and J. D. Pitts. 1988. Tissue and species conservation of the vertebrate and arthropod forms of the low molecular weight (16–18,000) proteins of gap junctions. *Cell Tissue Res.* 251:571–580.
31. Hertzberg, E. L. 1984. A detergent-independent procedure for the isolation of gap junctions from rat liver. *J. Biol. Chem.* 259:9936–9943.
32. Leitch, B., and M. E. Finbow. 1990. The gap junction-like form of a vacuolar proton channel component appears not to be an artifact of isolation—an immunocytochemical localization study. *Exp. Cell Res.* 190:218–226.
33. Páli, T., M. E. Finbow, A. Holzenburg, J. B. C. Findlay, and D. Marsh. 1995. Lipid-protein interactions and assembly of the 16-kDa channel polypeptide from *Nephrops norvegicus*. Studies with spin-label electron spin resonance spectroscopy and electron microscopy. *Biochemistry.* 34:9211–9218.
34. Uchida, E., Y. Ohsumi, and Y. Anraku. 1985. Purification and properties of H^+-translocating, Mg^{2+}-adenosine triphosphatase from vacuolar membranes of *Saccharomyces cerevisiae*. *J. Biol. Chem.* 260:1090–1095.
35. Marsh, D. 1982. Electron spin resonance: spin label probes. *In* Techniques in Lipid and Membrane Biochemistry, Vol. B4/II. J. C. Metcalfe and T. R. Hesketh, editors. *Elsevier.* B426-1–B426-44.
36. Marsh, D. 1985. ESR spin label studies of lipid-protein interactions. *In* Progress in Protein-Lipid Interactions, Vol. 1. A. Watts and J. J. H. H. M. de Pont, editors. Elsevier. Amsterdam. 143–172.
37. Horváth, L. I., P. J. Brophy, and D. Marsh. 1994. Microwave frequency dependence of ESR spectra from spin labels undergoing two-site exchange in myelin proteolipid membranes. *J. Magn. Reson.* B105:120–128.
38. Väänänen, H. K., E.-K. Karhukorpi, K. Sundquist, B. Wallmark, I. Roininen, T. Hentunen, J. Tuukkanen, and P. Lakkakorpi. 1990. Evidence for the presence of a proton pump of the vacuolar H^+-ATPase type in the ruffled borders of osteoclasts. *J. Cell Biol.* 111:1305–1311.
39. Thompson, J. D., D. G. Higgins, and T. J. Gibson. 1994. CLUSTAL W: improving the sensitivity of progressive multiple sequence alignment through sequence weighting, position-specific gap penalties and weight matrix choice. *Nucleic Acids Res.* 22:4673–4680.
40. Powell, G. L., P. F. Knowles, and D. Marsh. 1985. Association of spin-labeled cardiolipin with dimyristoylphosphatidylcholine-substituted bovine heart cytochrome *c* oxidase. A generalized specificity increase rather than highly specific binding sites. *Biochim. Biophys. Acta.* 816: 191–194.
41. Brotherus, J. R., O. H. Griffith, M. O. Brotherus, P. C. Jost, J. R. Silvius, and L. E. Hokin. 1981. Lipid-protein multiple binding equilibria in membranes. *Biochemistry.* 20:5261–5267.
42. Sachse, J.-H., M. D. King, and D. Marsh. 1987. ESR determination of lipid diffusion coefficients at low spin-label concentrations in biological membranes, using exchange broadening, exchange narrowing, and dipole-dipole interactions. *J. Magn. Reson.* 71:385–404.
43. King, M. D., J.-H. Sachse, and D. Marsh. 1987. Unconstrained optimization method for interpreting the concentration and temperature dependence of the linewidths of interacting nitroxide spin labels. Application to the measurement of translational diffusion coefficients of spin-labeled phospholipids in membranes. *J. Magn. Reson.* 72:257–267.
44. Whyteside, G., P. J. Meek, S. K. Ball, N. Dixon, M. E. Finbow, T. P. Kee, J. B. C. Findlay, and M. A. Harrison. 2005. Concanamycin and indolyl pentadieneamide inhibitors of the vacuolar H^+-ATPase bind with high affinity to the purified proteolipid subunit of the membrane domain. *Biochemistry.* 44:15024–15031.